Structural Dynamics

RESEARCH ARTICLE | FEBRUARY 09 2016

Identification of the dominant photochemical pathways and mechanistic insights to the ultrafast ligand exchange of $Fe(CO)_5$ to $Fe(CO)_4EtOH$

K. Kunnus; I. Josefsson; I. Rajkovic; S. Schreck; W. Quevedo; M. Beye; C. Weniger; S. Grübel; M. Scholz; D. Nordlund; W. Zhang; R. W. Hartsock; K. J. Gaffney; W. F. Schlotter; J. J. Turner; B. Kennedy; F. Hennies; F. M. F. de Groot; S. Techert; M. Odelius; Ph. Wernet; A. Föhlisch

Struct. Dyn. 3, 043204 (2016)
https://doi.org/10.1063/1.4941602

Identification of the dominant photochemical pathways and mechanistic insights to the ultrafast ligand exchange of $Fe(CO)_5$ to $Fe(CO)_4EtOH$

K. Kunnus,[1,2,a),b)] I. Josefsson,[3] I. Rajkovic,[4,c)] S. Schreck,[1,2] W. Quevedo,[1] M. Beye,[1] C. Weniger,[1] S. Grübel,[4,d)] M. Scholz,[4] D. Nordlund,[5] W. Zhang,[6,e)] R. W. Hartsock,[6] K. J. Gaffney,[6] W. F. Schlotter,[7] J. J. Turner,[7] B. Kennedy,[1] F. Hennies,[8] F. M. F. de Groot,[9] S. Techert,[4,10,11] M. Odelius,[3,a)] Ph. Wernet,[1,a)] and A. Föhlisch[1,2,a)]

[1]*Institute for Methods and Instrumentation for Synchrotron Radiation Research, Helmholtz-Zentrum Berlin für Materialien und Energie GmbH, Albert-Einstein-Strasse 15, 12489 Berlin, Germany*
[2]*Institut für Physik und Astronomie, Universität Potsdam, Karl-Liebknecht-Strasse 24/25, 14476 Potsdam, Germany*
[3]*Department of Physics, Stockholm University, AlbaNova University Centre, 10691 Stockholm, Sweden*
[4]*Max Planck Institute for Biophysical Chemistry, Am Fassberg 11, 37070 Göttingen, Germany*
[5]*Stanford Synchrotron Radiation Lightsource, SLAC National Accelerator Laboratory, Menlo Park, California 94025, USA*
[6]*PULSE Institute, SLAC National Accelerator Laboratory, Menlo Park, California 94025, USA*
[7]*Linac Coherent Light Source, SLAC National Accelerator Laboratory, Menlo Park, California 94025, USA*
[8]*MAX-lab, P.O. Box 118, 221 00 Lund, Sweden*
[9]*Department of Chemistry, Utrecht University, Universiteitsweg 99, 3584 CG Utrecht, The Netherlands*
[10]*Institute for X-ray Physics, Göttingen University, Friedrich Hund Platz 1, 37077 Göttingen, Germany*
[11]*Structural Dynamics of (Bio)Chemical Systems, DESY, Notkestrasse 85, 22607 Hamburg, Germany*

(Received 20 August 2015; accepted 22 January 2016; published online 9 February 2016)

We utilized femtosecond time-resolved resonant inelastic X-ray scattering and *ab initio* theory to study the transient electronic structure and the photoinduced molecular dynamics of a model metal carbonyl photocatalyst $Fe(CO)_5$ in ethanol solution. We propose mechanistic explanation for the parallel ultrafast intra-molecular spin crossover and ligation of the $Fe(CO)_4$ which are observed following a charge transfer photoexcitation of $Fe(CO)_5$ as reported in our previous study [Wernet et al., Nature **520**, 78 (2015)]. We find that branching of the reaction pathway likely happens in the $^1A_1$ state of $Fe(CO)_4$. A sub-picosecond time constant of the spin crossover from $^1B_2$ to $^3B_2$ is rationalized by the proposed $^1B_2 \rightarrow {}^1A_1 \rightarrow {}^3B_2$ mechanism. Ultrafast ligation of the $^1B_2$ $Fe(CO)_4$ state is significantly faster than the spin-forbidden and diffusion limited ligation process occurring from the $^3B_2$ $Fe(CO)_4$ ground state that has been observed in the previous studies. We propose that the ultrafast ligation occurs via $^1B_2 \rightarrow {}^1A_1 \rightarrow {}^1A'$ $Fe(CO)_4EtOH$ pathway and

[a)]Authors to whom correspondence should be addressed. Electronic addresses: kkunnus@stanford.edu; odelius@fysik.su.se; wernet@helmholtz-berlin.de; and alexander.foehlisch@helmholtz-berlin.de.
[b)]Present address: PULSE Institute, SLAC National Accelerator Laboratory, Menlo Park, California 94025, USA.
[c)]Present address: Stanford Synchrotron Radiation Lightsource, SLAC National Accelerator Laboratory, Menlo Park, California 94025, USA.
[d)]Present address: Swiss Light Source, Paul Scherrer Institut, 5232 Villigen PSI, Switzerland.
[e)]Present address: Ultrafast Optical Processes Laboratory, Department of Chemistry, University of Pennsylvania, Philadelphia, Pennsylvania 19104, USA.

the time scale of the $^1A_1$ $Fe(CO)_4$ state ligation is governed by the solute-solvent collision frequency. Our study emphasizes the importance of understanding the interaction of molecular excited states with the surrounding environment to explain the relaxation pathways of photoexcited metal carbonyls in solution.
[http://dx.doi.org/10.1063/1.4941602]

I. INTRODUCTION

The photochemistry and physics of transition metal coordination compounds reflect a complex array of electronic and nuclear dynamics occurring often on the ultrafast, femto- and picosecond time scales. Investigation of these processes at a molecular level has the potential of enhancing our understanding of chemical reactivity, but generally proves to be experimentally and theoretically challenging. Techniques with sub-picosecond time resolution and high sensitivity and selectivity to the metal center provide an important perspective with which to investigate organometallic photochemical dynamics. In comparison to numerous other spectroscopic methods, x-ray spectroscopy has the advantage of being element selective.[2] Combined with pump-probe schemes, it enables the evolution of the electronic structure to be followed with elemental and site specificity.[3] In recent years, time-resolved x-ray spectroscopy methods have been utilized to probe excited state molecular dynamics with (sub-)picosecond resolution.[1,4–12] This advancement has been mostly driven by technological progress in short-pulse x-ray sources and in particular, by recent developments of accelerator based light sources. In particular, femtosecond time-resolved resonant inelastic x-ray scattering (RIXS) experiments have become feasible at x-ray free-electron laser sources (XFELs).[1,10,13–16]

We report a femtosecond time-resolved RIXS investigation of the ligand exchange reaction dynamics triggered by the CO photodissociation from the transition metal complex $Fe(CO)_5$ in ethanol solution. The investigation presented here expands upon our earlier publication.[1] We studied the short time-scale dynamics (up to 3.5 ps after the excitation) of the reaction with 300 fs time resolution. Our approach employed RIXS at the Fe L_3 absorption edge (705–715 eV) which is selectively sensitive to the Fe 3d character of the valence states (i.e., the Fe electrons primarily involved in the bonding and chemical reactivity). This allowed us to resolve changes in the valence electronic structure of the iron carbonyl complex which relate to the Fe-CO bond dissociation, electronic exited state relaxation, and solvent bonding to the under-coordinated $Fe(CO)_4$ photoproduct.[1] Thereby, we can utilize not only the element-specificity of the x-ray probe to monitor the reaction center but also the ability of RIXS to discriminate different chemical species (coordination) and electronic states to map the evolution of the electronic structure with orbital specificity.

$Fe(CO)_5$ has a trigonal bipyramidal (D_{3h}) geometry and a closed shell, singlet A_1' electronic ground state. The onset of the optical absorption spectrum is at 3.5 eV.[17,18] The optical absorption cross section is dominated by transitions from orbitals of predominantly Fe 3d character to orbitals with significant CO 2π character, i.e., metal-to-ligand charge transfer (MLCT) excitations.[18–20] Absorption of a photon with 4.66 eV energy (266 nm) by $Fe(CO)_5$ is followed by a primary dissociation step which splits off one CO,[21–23] creating the $Fe(CO)_4$ photofragment with a quantum yield close to unity.[24] In the gas phase, $Fe(CO)_4$ undergoes further fragmentation with high quantum yield.[19,25–29] The time constant for this fragmentation was reported to be 3.3 ps.[30,31] In solution, depending on the excitation wavelength and the solvent, sequential dissociation can be suppressed,[21,22,32,33] but not necessarily eliminated.[34–37] Within the short time-scales studied here, the $Fe(CO)_4$ fragment is the relevant intermediate which interacts with the solvent and determines the course of the reaction.

It is well known that singlet $Fe(CO)_4$ is highly reactive and capable of ligand addition with a number of common organic compounds: alkanes, alkenes, alcohols, alkylphosphines, and alkylsilanes.[35,36,38–41] This reactivity arises from the fact that $Fe(CO)_4$ has an electron

deficiency at the Fe center; the 16 valence electrons do not fulfill the 18 electron rule. Furthermore, the Fe center is sterically free to interact with the solvent, making it a strong electrophile. The question thus arises whether the reactivity of $Fe(CO)_4$ towards solution modifies the exited-state relaxation pathways.[42] As reported in our earlier publication,[1] we concluded that after photodissociation of $Fe(CO)_5$, the reactive species $Fe(CO)_4$ converts from an excited singlet state to the triplet ground state and, in a parallel pathway, combines with an ethanol solvent molecule to form $Fe(CO)_4EtOH$ or geminately with CO to reform $Fe(CO)_5$ on a time scale of 200–300 fs. The aim of the present investigation is to detail these findings with particular emphasis on the mechanistic details of the reaction pathways.

An important aspect of $Fe(CO)_4$ reactivity relates to the spin state of the complex.[36,41] While singlet $Fe(CO)_4$ is highly reactive, the $^3B_2$ electronic ground state of $Fe(CO)_4$ does not coordinate with solvent.[42] The occurrence of $^3B_2$ $Fe(CO)_4$ is established in several solutions, but the mechanistic details of its creation had remained unresolved.[35,36,40,42] It was stated in the gas phase electron diffraction experiments by Ihee *et al.*[43] and Trushin *et al.* transient ionization experiment[31] that $Fe(CO)_4$ is created initially in a singlet state and that spin crossover (SC) must take at least several hundreds of picoseconds (according to Ryther *et al.* IR-absorption experiments even more than 200 ns (Refs. 28 and 29)). This interpretation of the gas phase studies differs significantly from the results of solution phase time-resolved IR-absorption studies, in which Snee *et al.* concluded that they observed triplet $Fe(CO)_4$ creation in less than 10 ps.[40,41]

The solvent environment can influence excited state dynamics in a variety of manners. Solvent polarity-dependent state shifts, solvent cage effects (geminate recombination), solvent assisted internal vibrational energy redistribution, and vibrational cooling (energy transfer to the solvent) can all play a significant role.[44–46] Here, we focus our main attention on the additional aspect of chemically specific coordination, namely, the coordination of ethanol to $Fe(CO)_4$, creating $Fe(CO)_4L$ (L = ligand, EtOH in case of ethanol solution). As mentioned earlier, Snee *et al.*[41] performed a series of experiments in different alcohol solutions and they observed ultrafast (<10 ps) formation of a hot triplet $Fe(CO)_4$ species, which is coordinated through a diffusive mechanism on the 42–340 ps time scale. Intriguingly, in contrast to other alcohol solutions, Snee *et al.* did not detect triplet $Fe(CO)_4$ in methanol solution (EtOH solution was not measured), possibly due to the difficulty in assigning the transient spectra to specific electronic states before the photoproducts have cooled vibrationally and the similar rate of solvent coordination and vibrational cooling in methanol. They speculated that in contrast to other alcohols, in methanol, $Fe(CO)_4$ could solvate at a faster rate and the observed 42 ps time constant could actually correspond to a cooling process. Recently, in a study by the same group, it was reported that the triplet $Fe(CO)_4$ intermediate was observed in methanol.[37] Specifically addressing $Fe(CO)_5$ photodissociation in ethanol using time-resolved Fe K-edge X-ray absorption spectroscopy, Ahr *et al.*[8] proposed that the electronic ground state interaction between ethanol and $Fe(CO)_5$ influences the excited state dynamics of $Fe(CO)_5$, making the removal of CO and the addition of EtOH as concerted processes. Creation of $Fe(CO)_4EtOH$ was not resolved with the time resolution of the experiment of 3 ps, but they deduced a 14 ps cooling rate. They did not discuss the spin state of the photofragment and assumed it to be a singlet throughout the process. Their model was supported with the argument that in solution a weak $Fe(CO)_5$-EtOH complex is formed.[47,48]

It is evident that a number of questions related to the mechanism of $Fe(CO)_5$ photodissociation in solution and in particular, the related ligand substitution reactions remain unresolved despite extensive prior study. What is the pathway leading to triplet $Fe(CO)_4$ in solution? What are the mechanistic details of the $Fe(CO)_4$ ligand addition reaction and how can we explain the timescale? How in detail can the findings for the short sub-ps time scale[1] be reconciled with the results for longer time scales?[36,37,41,49] We aim to address these questions below.

II. METHODS

A. Experimental details

The experiment was conducted at the LCLS Soft X-ray Materials Science (SXR) beamline[50,51] with the Liquid Jet Endstation. A detailed description of the endstation can be found

elsewhere.[52] The experiment was performed on a 1M $Fe(CO)_5$ ethanol solution. The third harmonic of a Ti:sapphire laser system at 266 nm (4.66 eV) was used for the initiation of the photoreaction. The laser pulse length was 100 fs and estimated pulse energy was $\sim 5\,\mu$J (peak fluence $\sim 1.25 \times 10^{11}$ W/cm^2). We found the total time resolution of the experiment to be 300 fs full width at half maximum (FWHM) mainly determined by the relative time-of-arrival jitter between the optical laser and the FEL x-ray pulses (deduced from the experimental time traces) and the x-ray pulse length of 160 fs. RIXS spectra were measured at the Fe L_3-edge (705–715 eV) with an excitation bandwidth of 0.5 eV.[53] Resolution of the RIXS spectra, defined by the diameter of the jet (20 μm) in the "slitless" mode, was 1.0 eV. The average peak incident fluence of the x-ray beam was 2×10^{11} W/cm^2 (1.6×10^{10} photons per pulse). Further details can be found in Ref. 1.

B. Computational details

Accurate simulations of L-edge x-ray spectra require inclusion of relativistic effects and a balanced treatment of many core- and valence-excited states.[54–58] For these reasons, theoretical x-ray spectra were derived from restricted active space self-consistent field (RASSCF) calculations.[59] The active space in the RASSCF calculations included 14 electrons in 14 orbitals; the 2p in the RAS1 space with at most one hole, four 3d in the RAS2 space and in RAS3 seven orbitals, including the nominally empty 3d orbital and the lowest unoccupied e′, e″ and e′ orbitals depicted in Fig. 1, with at most 2 electrons. Recently, also Suljoti *et al.* applied the RASSCF method to $Fe(CO)_5$.[60] Further computational details can be found in Ref. 1.

RIXS spectra were simulated using the Kramers-Heisenberg formula.[61] Spectra were calculated for an ensemble of randomly oriented molecules excited by linearly polarized light and detected in the plane of polarization.[62] Interference effects were excluded. To account for intermediate state lifetime broadening at the L_3 and L_2 edges, the values of 0.3 eV and 0.6 eV (FWHM) were used, respectively.[63] The bandwidth of the incident photons was 0.5 eV FWHM

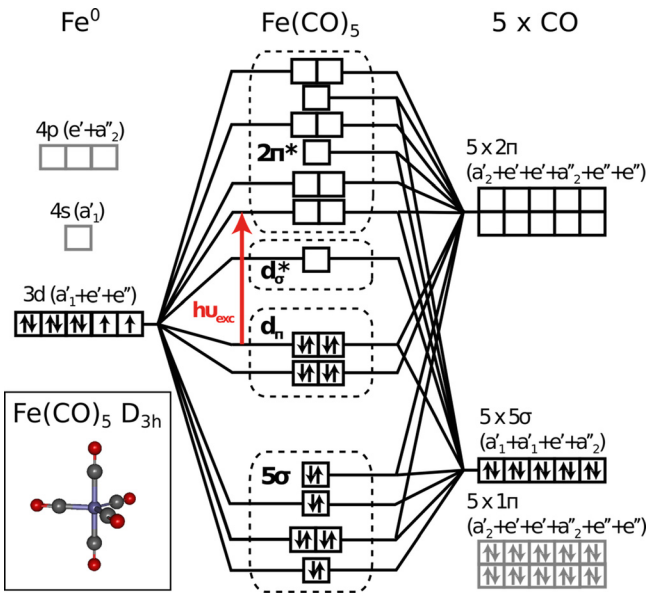

FIG. 1. Qualitative valence molecular-orbital (MO) diagram of $Fe(CO)_5$. Displayed is the subset of $Fe(CO)_5$ MOs which are derived from Fe 3d and CO 5σ and 2π orbitals. For the sake of clarity, the MOs with mostly Fe 4s, 4p, and CO 1π character are not shown (depicted for completeness in gray). The labels for the respective symmetry adapted orbitals in the D_{3h} point group are given in the parentheses after the Fe and CO orbital labels. MOs contributing most to Fe-CO bonding are additionally combined in four groups and labeled based on their symmetry with respect to the Fe-CO bond and the metal/ligand character (bold labels). Photoexcitation initiated by the 266 nm (4.66 eV) laser photons corresponds to MLCT transitions between occupied d_π and unoccupied $2\pi^*$ MOs (red arrow). The inset shows the $Fe(CO)_5$ ground state geometry (atoms are colored accordingly: blue—Fe, gray—C, and red—O).

(Gaussian). RIXS spectra were also broadened with the spectrometer resolution (1 eV FWHM, Gaussian). Finally, a 0.5 eV Gaussian broadening was applied for both intermediate and final states to account for additional broadening observed in the experiment, most likely due to inhomogeneous broadening from solvent environment and vibrational effects.[64,65]

Ab initio Car-Parrinello molecular dynamics (CPMD) simulation[66] within the periodic density functional framework were performed for 25 ps (7 ps equilibration) on the $Fe(CO)_5$ complex solvated by 100 ethanol at a density of 0.785 g/cm^3 and ambient temperature, obtained through the Nose-Hoover thermostat coupling at 3000 cm^{-1}. The system was deuterated and a time-step of 0.1 fs was used in combination with a fictitious electron mass of 300 a.u. in the Car-Parrinello dynamics.[67] The CPMD simulation was initialized from a 1 ns long classical MD simulation (MDynaMix) using a rigid solute with the Charmm force field[68] and the OPLS-AA force field for ethanol.[69] We used the Perdew-Burke-Ernzerhof (PBE) functional augmented with empirical van der Waal interactions[70] and a 85 Ry kinetic energy cut-off of the plane-wave expansion. We employed norm-conserving pseudo-potentials[71] derived for the PBE functional for all atoms except iron, for which we used an 8-electron GTH pseudo-potential[72] developed for the Pade functional.

III. RESULTS

The results of the time-resolved RIXS (tr-RIXS) measurements are summarized in Fig. 2. Panel (a) displays the pumped-unpumped difference RIXS map. One notices a decrease in the $(2p_{3/2})^{-1}(2\pi^*)^1$ resonance at 711.5 eV, a small increase of $(2p_{3/2})^{-1}(d_\sigma^*)^1$ resonance at 709.5 eV, and a larger increase from 706 to 709 eV where the $Fe(CO)_5$ ground state has no absorption. Different from Ref. 1, we define in Fig. 2(a) five spectral regions (1, 2, 2b, 3, and 4) and not four (1, 2, 3, and 4). We use delay scans taken in these regions (Fig. 2) to investigate the dynamical pathway of the reaction.

Identification and assignments of the species observed in the experiment are based on a comparison of the experimental tr-RIXS data (Fig. 2) with the RIXS maps calculated for various possible geometries and electronic states (Fig. 3 and Figs. S4–S13). As detailed in our previous publication,[1] minimally three distinct photoproducts are required to explain the experimental intensities. Here, this assignment is briefly summarized because the following discussions and analyses are based on it. The three species identified in Ref. 1 are labeled as E, T, and L. E stands for a "hot" singlet excited state of the $Fe(CO)_4$ photoproduct, T for vibrationally "hot" lowest triplet state ($^3B_2$) $Fe(CO)_4$, and L for "hot" ligated singlet ($^1A_1$) $Fe(CO)_4$, i.e., a mixture of the singlet ground state of $Fe(CO)_4EtOH$ (species C) and $Fe(CO)_5$ (species H). Extending our previous assignments, we discuss below the involvement of an additional species S, a vibrationally "hot" singlet state $Fe(CO)_4$. Descriptions and assignments of the species E, T, S, C, H, and L are summarized in Table I. Further details on the assignments of the photoproducts can be found in the supplementary material. We construct two consistent rate models that describe the observed experimental intensities in the five regions defined in Fig. 2. Relative intensities (contrasts) of the species in all five regions were extracted from the calculated RIXS map in Fig. 3 and kept fixed during the fitting procedure. (The details about the rate model can be found in the supplementary material.)

First kinetic rate model is same as in Ref. 1. (The results of this rate model are displayed in Fig. 2(b).) This kinetic rate model includes two parallel reaction pathways, E → T and E → L. This is the simplest rate model which can show reasonable agreement with the experiment (Fig. 2(b)). However, in the gas phase, it has been shown that the $^1B_2$ state of $Fe(CO)_4$ (species E) relaxes ultrafast to the singlet closed shell $^1A_1$ state (species S).[31] In addition, species S is reactive towards ligand addition, which, as we will argue below, provides possible explanation to ultrafast appearance of species L. Therefore, we will consider here a second kinetic rate model which includes E → S relaxation, followed by parallel S → T and S → L pathways. Fit of the corresponding rate model is shown in Fig. 2(c). Similarly to the first rate model, it is able to fit the experimental delay scans with a good accuracy. The extracted time constants for both kinetic rate models are listed in Table II. We would like to emphasize that the two models are not

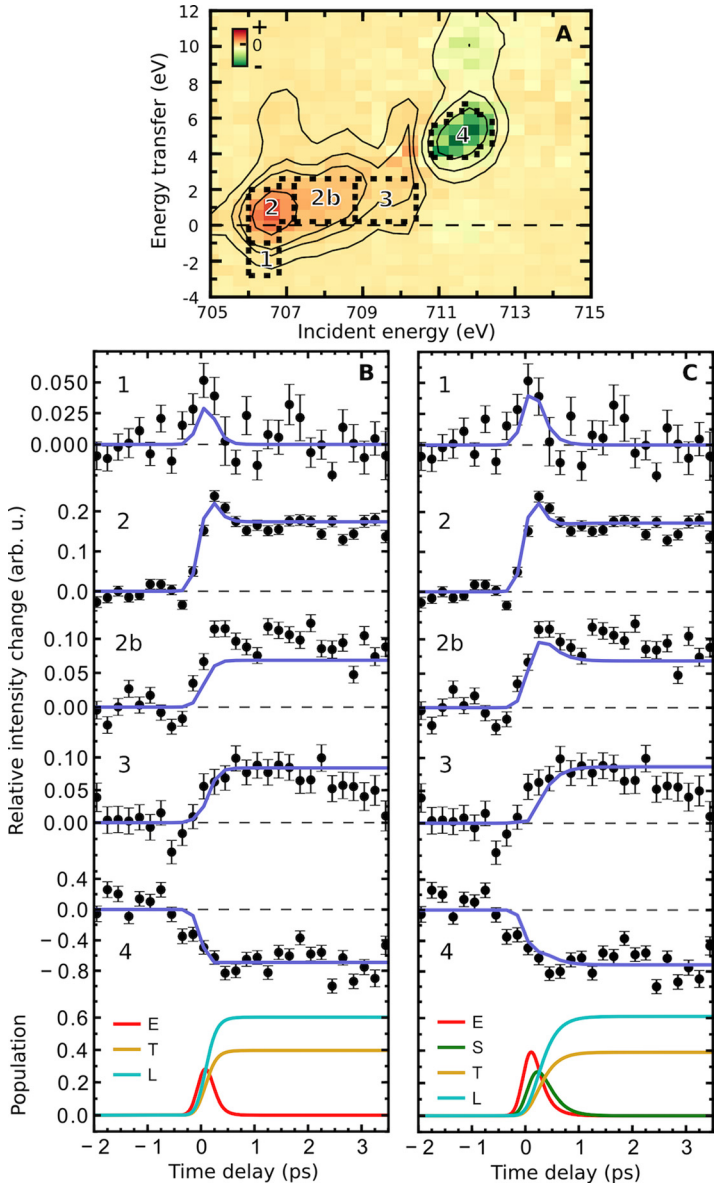

FIG. 2. Time-resolved experimental RIXS data and kinetic model fit. (a) Pumped-unpumped difference RIXS map; (b) kinetic rate model fits (solid lines) of experimental delay scans (black circles, error bars length is one standard deviation to each side) with three photoproducts E, T, and L; and (c) with four photoproducts E, S, T, and L. Experimental delay scans are from regions shown in the difference RIXS map (labeled with numbers). Relative population dynamics of the photoproducts resulting from the fits are also displayed.

contradictory. Both models describe the branching of species E to T and L; however, the second model introduced here elaborates the "minimal" model applied in Ref. 1 by including a new intermediate species S. Below we turn to a detailed discussion of the proposed reaction pathways with a particular emphasize on the possible participation of species S, a singlet closed shell singlet state of $Fe(CO)_4$.

IV. DISCUSSION

Fig. 4 summarizes schematically the relevant potential energy surfaces (PESs) and pathways of $Fe(CO)_5$ photoreaction in ethanol. The relative energies of particular molecular geometries and electronic states are calculated using RASSCF and CASPT2 methods (Table S3).[73] The qualitative PESs in Fig. 4 are constructed based on the previous studies.[31,36,41,74] Based on

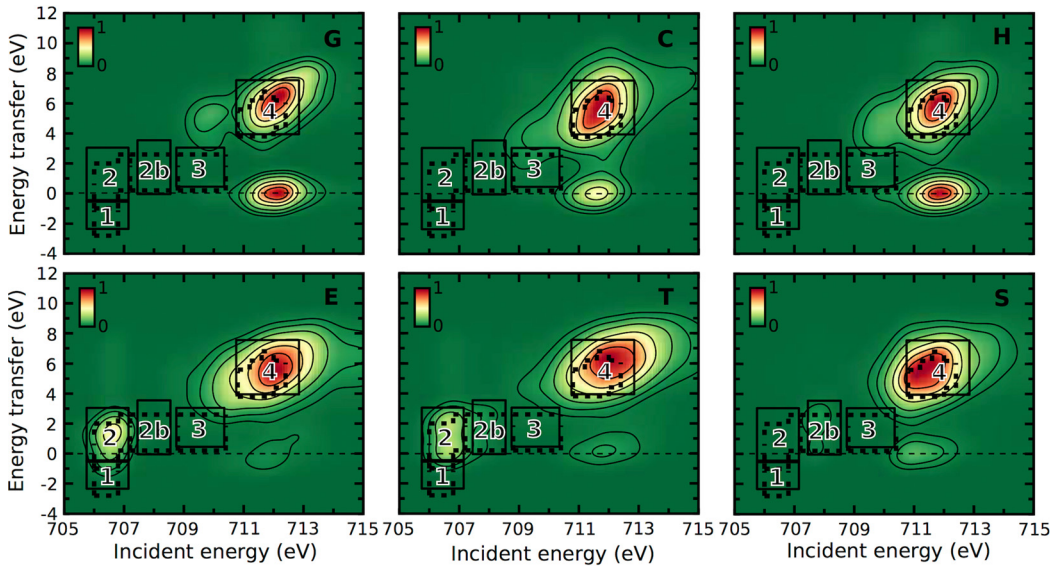

FIG. 3. Calculated RIXS maps of the relevant species. Species are defined in Table I. Thick dashed lines show regions used to extract experimental delay scans (same as in Fig. 2(a)) and thin solid lines show regions used to extract intensity contrasts of the different species for use in the rate model.

these PESs, we proceed with discussing the mechanistic details of the experimentally observed dynamical pathways.

A. $Fe(CO)_5$ photodissociation

Based on the previous studies, it is known that $Fe(CO)_5$ dissociates on an ultrafast (<100 fs) time scale.[25,26,31] The effectively instantaneous (within our 300 fs time resolution) appearance of the ligand field (LF) $^1B_2$ excited state $Fe(CO)_4$ (species E) after the photoexcitation of

TABLE I. Assignment of species and definitions based on the calculations. For further details, see the supplementary material. Calculated RIXS maps of the species are displayed in Fig. 3.

Species	Description	Geometry and electronic state	Regions with significant intensity
E	"Hot" singlet excited state $Fe(CO)_4$	$Fe(CO)_4T$, $^1B_2$ (LF)	1, 2, 3, 4
		$Fe(CO)_4S$, $^1B_2$ (LF)	
		$Fe(CO)_4E$ $^1B_2$ (LF)	
T	"Hot" lowest triplet state $Fe(CO)_4$	$Fe(CO)_4T$, $^3B_2$ (LF)	2, 2b, 4
		$Fe(CO)_4S$, $^3B_2$ (LF)	
		$Fe(CO)_4E$ $^3B_2$ (LF)	
S	"Hot" lowest singlet state $Fe(CO)_4$	$Fe(CO)_4T$, $^1A_1$ (GS)	2b, 4
		$Fe(CO)_4S$, $^1A_1$ (GS)	
		$Fe(CO)_4E$ $^1A_1$ (GS)	
C	"Hot" singlet ground state $Fe(CO)_4$EtOH complex	$Fe(CO)_4$EtOH-B, $^1A'$ (GS)	3, 4
		$Fe(CO)_4$EtOH-C, $^1A'$ (GS)	
H	"Hot" singlet ground state $Fe(CO)_5$	$Fe(CO)_5$, $^1A_1$ (GS)	3, 4
		$Fe(CO)_5C2v90$, $^1A_1$ (GS)	
		$Fe(CO)_5C_{4v}120$, $^1A_1$ (GS)	
		$Fe(CO)_5C_{4v}180$, $^1A_1$ (GS)	
L	"Hot" singlet ground state ligated $Fe(CO)_4$	C	3, 4
		H	

TABLE II. Time constants deduced from the rate model analysis. See Figs. 2(b) and 2(c) for a comparison of the two rate models.

Model without species S		Model with species S	
	Time constant (fs)		Time constant (fs)
E → T	300 ± 100	E → S	200 ± 100
E → L	200 ± 100	S → T	400 ± 100
		S → L	300 ± 100

$Fe(CO)_5$ to the MLCT states is a result of several very fast internal conversion (IC) processes which also include dissociation of a CO. Such ultrafast excited-state dynamics in $Fe(CO)_5$ is facilitated by the many energetically close lying states and the Jahn-Teller effect present in states with E′ orbital symmetry (Fig. 4). Trushin *et al*. deduced from their gas phase experiment three time constants leading to excited singlet $Fe(CO)_4$.[31] Two time constants before the dissociation, 21 fs and 15 fs, were interpreted as electronic relaxations in MLCT and LF manifolds (summarized as a single electron back-transfer process in Fig. 4) which are then followed by the dissociation on $^1B_2$ surface within 30 fs. These time scales are consistent with the effectively instantaneous appearance of the excited $Fe(CO)_4$ (species E) in our experiment. In addition, our observation of the $^1B_2$ state is consistent with the dissociation in the singlet manifold. However, given our data quality and time-resolution, we cannot completely exclude alternative dissociation pathways, e.g., dissociation in the triplet manifold. Also, we find it possible that the dissociation happens directly from some MLCT state. Similarly to ligand field $^1E'$ states, the dipole allowed MLCT $^1E'$ states are subjects to a Jahn-Teller effect. Such a dissociation pathway would lead to the respective $Fe(CO)_4$ MLCT state(s), which would then internally relax to the LF $^1B_2$ state. Distinguishing between LF and MLCT dissociation pathways requires improved experimental time resolution.

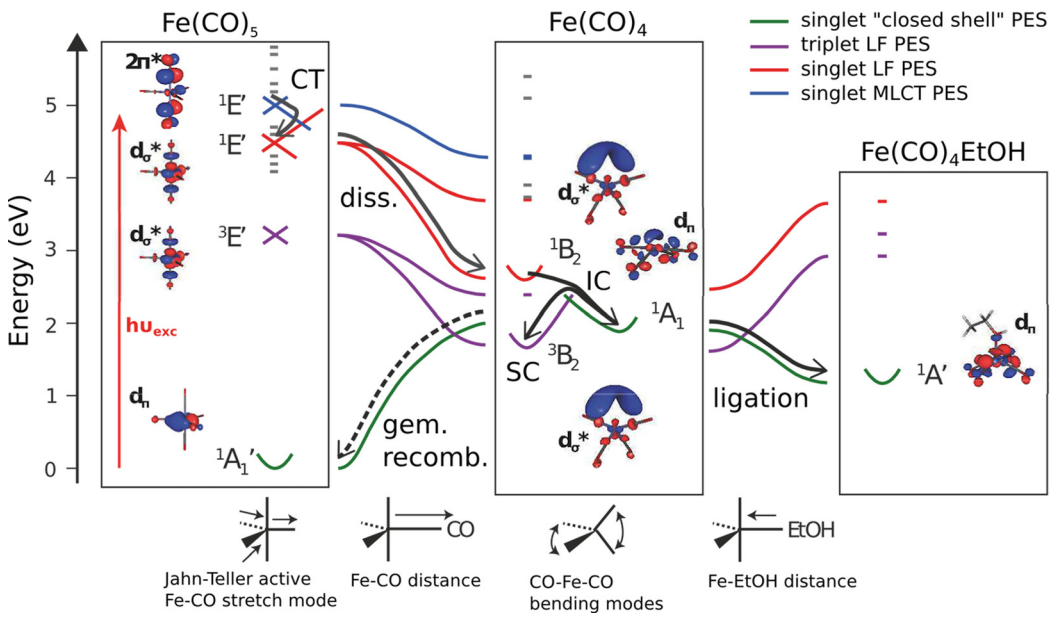

FIG. 4. Schematic pathways of $Fe(CO)_5$ photoreaction in ethanol. Illustrative MOs populated by the "active" electron for each state is shown next to the state label. Relative state energies of the displayed geometries are from RASSCF/CASPT2 calculations. Shown potential energy surfaces (PESs) are qualitative. Charge back-transfer (CT) and dissociation processes are not directly observed in this work and therefore depicted with gray arrows. Geminate recombination is a minority channel and thus represented by a dashed arrow.

Due to insufficient time resolution, we can neither confirm nor exclude the influence of the solvent before or during the dissociation of CO, corresponding to the recently proposed concerted CO dissociation and EtOH addition mechanism by Ahr *et al.*[8] Our kinetic rate model analysis (Table II.) demonstrates that the experimental findings are consistent with all photodissociated molecules converting to the four-coordinated $^1B_2$ state of $Fe(CO)_4$ (species E), consistent with the interpretation of the gas phase measurements of Trushin *et al.*[31] However, our observation of subsequent ultrafast ligation of species E agrees with the claimed ultrafast appearance of $Fe(CO)_4EtOH$ complex by Ahr *et al.*,[8] although the observation of four-coordinated $^1B_2$ intermediates by us requires an EtOH addition mechanism which is not concerted with CO dissociation. Below we therefore discuss in detail the possible mechanisms of ultrafast ligation of species E which are sequential to CO dissociation and which do not require a presence of six-coordinate $Fe(CO)_5EtOH$ complexes prior to photoexcitation. However, we will show below that physical mechanism of ultrafast ligation requires the presence of the species S (Fig. 2(c)), augmenting the model introduced in Ref. 1 that does not include the species S (Fig. 2(b)).

B. $Fe(CO)_4$ spin crossover

Decay of the $^1B_2$ $Fe(CO)_4$ state (species E) to the $^3B_2$ triplet ground state (species T) takes ~300 fs.[1] Such fast SC time scales has now been observed in variety of coordination and organometallic complexes and appears to be the rule, rather than the exception for metal complexes.[75–78] To the best of our knowledge, this reported time scale for the intramolecular SC in $Fe(CO)_4$[1] has not been measured before, although the (ultra)fast appearance of triplet intermediates in these systems has been previously detected.[35,40,41]

Our experimental data are consistent with two SC mechanisms: direct SC from $^1B_2$ to $^3B_2$ (E → T) or IC from $^1B_2$ to $^1A_1$ followed by SC from $^1A_1$ to $^3B_2$ (E → S → T). The first option, corresponding to the first rate model used in Ref. 1, would correspond to a spin-flip transition without a change in orbital character. This direct SC is, however, unlikely because it violates the energy gap rule (see also respective PESs in Fig. 4). In addition, according to Trushin *et al.*, the IC from $^1B_2$ to $^1A_1$ takes only 50 fs, reasonably agreeing with the extracted time constant 200 ± 100 fs. Besora *et al.* calculated the $^3B_2$ to $^1A_1$ hopping probability to be 1/13 resulting from the spin-orbit coupling of these states.[36] Given that spin allowed surface hopping from $^1B_2$ to $^1A_1$ is 50 fs,[31] it is thus reasonable to conclude that the spin-forbidden surface hopping (SC) from $^1A_1$ to $^3B_2$ is on the order of ~500 fs, therefore, rationalizing the experimentally observed 400 fs time scale. Therefore, we find that the presence of ultrafast SC can be explained by evoking the intermediate S as in the second kinetic rate model (Fig. 2(c) and Table II). The population of an intermediate $^1A_1$ state (i.e., species S) also matches with the observed ultrafast ligand addition pathway, as we will argue below. Further studies of the $Fe(CO)_4$ potential energy surfaces and the determination of the minimum energy crossing points between the $^1B_2$, $^1A_1$, and $^3B_2$ surfaces could give additional valuable insight to the proposed SC pathway.

C. Ultrafast ligation of $Fe(CO)_4$

The surprisingly fast time scale for the solvent addition of 200–300 fs demonstrates the high reactivity of $Fe(CO)_4$. In order to understand this high bimolecular reaction rate, we consider two factors: the collision frequency and the ratio of reactive/non-reactive collisions. The time constant of ligation is on the same order of magnitude as the average solute-solvent collision frequency of ~500 fs, indicating that effectively every collision with the solvent is reactive. The collision frequency was deduced by assuming a collision radius of 2 Å for both $Fe(CO)_5$ and EtOH at room temperature ($kT = 0.0257$ eV). Additionally, 500 fs is also the time it takes to travel 2 Å with an average relative solute-solvent velocity at room temperature. 2 Å is the distance molecules need to move to form a $Fe(CO)_4EtOH$ complex: The distance from the Fe center to oxygen or carbon of an EtOH molecule in the first solvation shell is ~4 Å and ~5 Å (Fig. 5), respectively, and the corresponding bond length in a hydroxyl bound $Fe(CO)_4EtOH$ complex is ~2 Å and in a alkyl bound $Fe(CO)_4EtOH$ complex is ~3 Å.[73]

Although the observed ligation time constant matches well, within the experimental errors, with the room temperature collision frequency of 500 fs, it is important to consider if a considerable excess of vibrational energy in the $Fe(CO)_4$ fragment could have an effect on the ligation time constant because there is an obvious square root dependence between the speed of a molecule and the kinetic energy. From gas phase studies, it is known that $Fe(CO)_4$ has to accommodate about 2.2 eV excess vibrational energy directly after dissociation (depending on the exact electronic state).[79] However, at such early time delays, it is difficult to estimate the amount of vibrational energy in modes relevant for the ligation because there has not been enough time for thermalization of the energy through internal energy redistribution processes. At so early times, a considerable fraction of the 2.2 eV energy is carried by CO-Fe-CO bending motions that are strongly coupled to CO dissociation coordinate.[79] It is nevertheless evident that even if a small fraction of this energy is deposited to the $Fe(CO)_4$ translational degrees of freedom, the ligation time constant could shorten considerably. Given the experimentally observed time constant, one could quantify that the translational energy of $Fe(CO)_4$ is in the order of 0.1 eV or less.

Ligation at the rate of the collision frequency is only possible if all of the $Fe(CO)_4$ collisions with the solvent are reactive, resulting in the formation of the complex effectively during a first collision. It follows that there must be no hindrance of the ligation neither due to slower dynamics of ethanol reorientation and/or hydrogen-bond network rearrangements nor due to IC from the open shell $^1B_2$ state to the closed shell $^1A_1$ (or $^1A'$ in C_s symmetry) state. We shall discuss these two aspects in more detail.

IC to $^1A_1$ $Fe(CO)_4$ state is necessary for the ligand addition reaction because only the $^1A_1$ state is reactive with respect to ligation (i.e., $^1A_1$ potential energy surface is barrierless and attractive, Fig. 4). This is distinctive from the open shell $^{1,3}B_2$ LF states which are repulsive

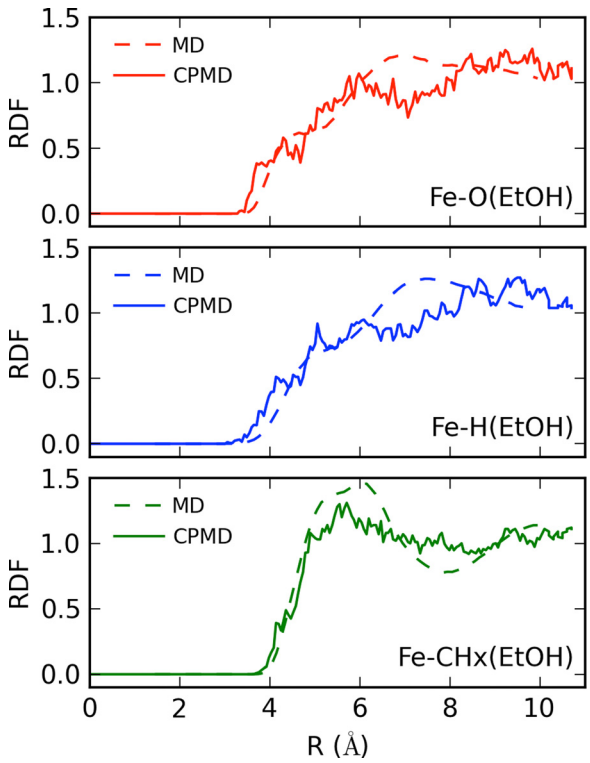

FIG. 5. Calculated radial distribution functions of some relevant atomic distances between solute $Fe(CO)_5$ and solvent EtOH. First solvation shell O(EtOH) is ∼4 Å from Fe and second solvation shell O(EtOH) is about ∼6 Å from Fe. Details of the classical molecular dynamics (MD) and Car-Parrinello molecular dynamics (CPMD) simulations can be found in Section II.

(Fig. 4). The latter can be explained by the fact that the low-energy anti-bonding d_σ* orbital which strongly hybridizes with the occupied orbitals of the incoming ligand is unoccupied in $^1A_1$ in contrast to $^{1,3}B_2$ states.[1] Addressing a possible hindrance of ligation due to IC from the $^1B_2$ surface to the $^1A_1$ surface, it is important to discuss the location of surface hopping. We consider it unlikely that the hopping takes place along the Fe-EtOH distance coordinate because the $^1A_1$ and $^1B_2$ surfaces do not cross along this coordinate (Fig. 4). Most likely, it is the very energetic internal CO-Fe-CO bending modes that are active in IC from $^1B_2$ to $^1A_1$ (Fig. 4). The surface hopping could take place at a tetrahedral $Fe(CO)_4$ geometry where $^1B_2$ and $^1A_1$ states are degenerate.[31] The high internal energy contained by the CO-Fe-CO bending modes allows the molecule to access the crossing seams between $^1B_2$ and $^1A_1$ promptly. As mentioned before, Trushin *et al*. measured a time constant of 50 fs for this process, and therefore $Fe(CO)_4$ molecules convert to reactive $^1A_1$ state already before colliding with the solvent.[31] Therefore, we find that ultrafast ligation can be present only if the $Fe(CO)_4$ converts ultrafast to intermediate S species, again favoring the second kinetic rate model (Fig. 2(c)) in contrast to the first kinetic rate model introduced in Ref. 1 (Fig. 2(b)).

Experimental and computational studies have shown that (equilibrium) reorientational dynamics in bulk ethanol occur on time scales on the order of 10–100 ps.[80–82] Efficient ligation of $^1A_1$ $Fe(CO)_4$ species can therefore be possible only if the ethanol molecules in the first solvation shell of $Fe(CO)_5$ are "pre-aligned" to a favorable configuration for the reaction (i.e., with hydroxyl groups towards $Fe(CO)_5$) or if the ligation is not sensitive to the orientation of ethanol molecules. In a recent study, it was found that in $Fe(CO)_5$ ethanol solution a $Fe(CO)_5$EtOH complex can be formed.[48] Our calculations failed to find a stable $Fe(CO)_5$EtOH complex, but we confirmed the presence of an ordered first solvation shell with ethanol molecules oriented towards $Fe(CO)_5$ with their hydroxyl groups (Fig. S20).[73] The presence of pre-oriented solvent molecules is favorable for ultrafast ethanol addition reaction. Alternatively, our time resolved RIXS spectra do not distinguish between hydroxyl and alkyl coordinated ethanol molecules. Therefore, based on the current experiment, we cannot conclude on how important the ordering of the solvation shell is for the ligation. However, we find that pre-orientation is not necessary to explain our experimental observables. Highly reactive $^1A_1$ $Fe(CO)_4$ species can also react with alkyl groups,[35,83] creating an agostic-type of bond[84] with the methyl group of ethanol. Thus, we assume that both hydroxyl and alkyl solvated complexes are created in the process (species C was defined before as 1:1 mixture of hydroxyl and alkyl solvated $Fe(CO)_4$EtOH complexes). The fact that reorientation of the solvent molecules or a disruption of the hydrogen-bond network does not seem necessary thus explains why ligation of $^1A_1$ $Fe(CO)_4$ molecules (species S) with the solvent is so fast.

We performed two CPMD simulations to investigate the solvation of $Fe(CO)_4$. Simulations were performed by removing one CO ligand at $t = 0$ from a $Fe(CO)_5$ molecule in $^1A'_1$ closed shell ground state (Fig. 6). Therefore, different from the situation in the experiment, there is no excess vibrational energy deposited to $Fe(CO)_4$ moiety. Note that in both simulations the EtOH molecule which eventually binds with the $Fe(CO)_4$ comes from a second solvation shell. This could be one reason why in these two simulated cases the ligand addition takes ~4 ps, i.e., significantly more than observed in the experiment. Although these simulation do not directly confirm the experimental findings, they nevertheless show that the reduction of Fe-O(EtOH) distance by 2 Å can happen with less than 1 ps even in case of cold $Fe(CO)_4$, therefore supporting our argument based on the solute-solvent collision frequency.

The ultrafast ligand addition mechanism proposed here is qualitatively similar to solvation of $Cr(CO)_5$ after photodissociation of $Cr(CO)_6$ in alcohol solution. First observed by Simon *et al*. with UV/Vis transient absorption spectroscopy, in methanol solution, a $Cr(CO)_5$MeOH is created with ~2.5 ps.[85] Joly *et al*. carried out measurements in a selection of alcohols (including ethanol) and found a rather solvent independent 1.6 ps solvation time constant which is preceded by 350 fs dissociation.[86,87] The initially created $Cr(CO)_5$ROH species are mostly alkyl coordinated, rearrangement to thermodynamically stable hydroxyl coordinated species takes 80–200 ps, depending on the solvent.[88–90] Note that, in contrast to $Fe(CO)_4$, the ground state of

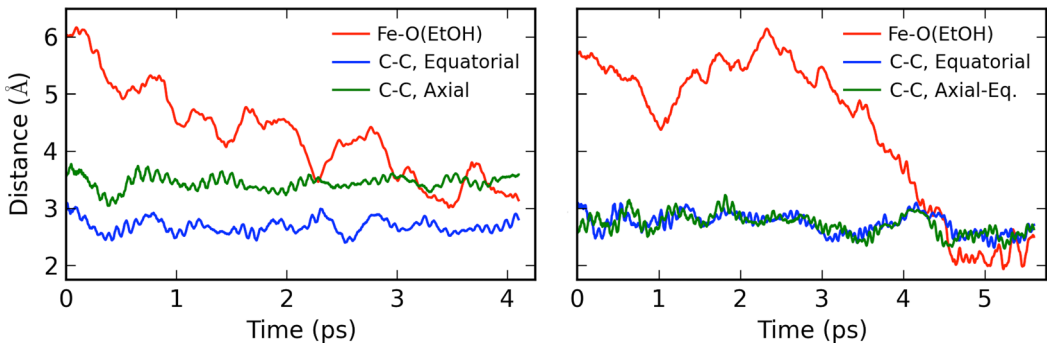

FIG. 6. Left: *Ab initio* Car-Parrinello molecular dynamics (CPMD) simulation of solvation of a cold $^1A_1$ $Fe(CO)_4$ state followed by removal of one equatorial CO from $Fe(CO)_5$. In addition to Fe-CO(EtOH) distance, also the C-C distances of two remaining CO pairs are shown. Right: CPMD simulation of solvation of a cold $^1A_1$ $Fe(CO)_4$ state followed by the removal of one axial CO from $Fe(CO)_5$. In addition to Fe-CO(EtOH) distance, also the C-C distances of two remaining CO pairs are shown.

$Cr(CO)_5$ is a singlet and therefore the $Cr(CO)_5$ species follow the ultrafast ligation pathways without any competing branching to a triplet state. The slower time scale of $Cr(CO)_5$ ligation compared with $Fe(CO)_4$ could be related to the additional CO ligand which sterically hinders the reaction.

The E → L reaction can thus be summarized in two steps (Fig. 4). First, intra-molecular $^1B_2$ to $^1A_1$ IC facilitated by the very energetic CO-Fe-CO bending modes, which is followed by a single collision with the solvent on an attractive $^1A_1$ ($^1A'$ in C_s symmetry) surface with an approximately room temperature solute-solvent collision speed (Fig. 4). We therefore propose that branching of the $Fe(CO)_4$ relaxation pathway takes place in the four-coordinated $^1A_1$ state. Which pathway a particular molecule takes depends on what happens before: reactive collision with the solute or SC to $^3B_2$ driven by highly energetic CO-Fe-CO bending motions. In Section II B, we proposed a mechanism for SC which explains why the latter has a similar time scale to the solute-solvent collision frequency, therefore rationalizing our experimental observation that both SC and ligation are relevant channels.

Snee *et al.* studied slower time scale kinetics (up to 700 ps) of the $Fe(CO)_5$ photoreaction in methanol and they observed the appearance of CO stretch peaks of the thermally relaxed $Fe(CO)_4$MeOH complex with a time constant of 42 ps.[41] We believe that such slow formation of the final reaction product is consistent with the ultrafast ligand capture process observed here. As noted by Snee *et al.*, the slow time scale is related to cooling of the $Fe(CO)_4$ moiety, diffusional reorientation motions of the solvent molecules, and reaction of the remaining triplet $Fe(CO)_4$ species with ethanol. This could also include relaxation of alkyl solvated $Fe(CO)_4$EtOH complexes to hydroxyl bound configurations, similar to $Cr(CO)_5$ROH. Consistently, vibrational relaxation of the CO-Fe-CO bending modes has been independently measured to take 10–20 ps, depending on the solvent.[8,91,92] We would therefore emphasize that the ultrafast ligation process identified here does not lead to a formation of stable $Fe(CO)_4$EtOH complex with a single clearly defined structure corresponding to the minimum energy geometry. Instead, the observed spectroscopic signature of the complex indicates that a solvent molecule has moved to the first coordination shell of iron. The formed solvent complex thus samples likely a wide range of geometries that have a solvent molecule in proximity to iron.

V. SUMMARY AND OUTLOOK

Our study complements and details our earlier publication on the excited-state dynamics of $Fe(CO)_4$ after CO photodissociation of $Fe(CO)_5$ in ethanol solution.[1] By analyzing in detail the experimental results and corresponding quantum-chemical calculations, we reveal that chemical interaction between $Fe(CO)_4$ and the surrounding environment significantly modifies the excited

state relaxation pathways on the sub-picosecond time scales. This is manifested by the parallel appearance of four-coordinated triplet and five-coordinated (ligated) singlet photoproducts. Based on an extensive kinetic rate model analysis, we propose the following reaction pathways. Photodissociation of $Fe(CO)_5$ yields the $Fe(CO)_4$ photoproduct in a ligand-field excited state ($^1B_2$). Relaxation of this state follows two competing pathways: Approximately half of the $Fe(CO)_4$ molecules undergo a spin crossover to the $^3B_2$ state, while the other half relaxes via the formation of a solute-solvent complex, $Fe(CO)_4EtOH$ in the $^1A'$ ground electronic state, or recombines with the CO to form $Fe(CO)_5$. We propose that both SC and ligation happen via four-coordinated $^1A_1$ state that is populated ultrafast due to highly energetic CO-Fe-CO bending motions. The branching of the reaction pathway happens in the $^1A_1$ state: it can convert into non-reactive $^3B_2$ state, facilitated again by the CO-Fe-CO bending motions, or it can collide with a solvent molecule and form a $Fe(CO)_4EtOH$ complex. Due to the extremely high reactivity of the $Fe(CO)_4$ $^1A_1$ state, ligation does not require considerable reorientation of solvent molecules and therefore $Fe(CO)_4$ in the $^1A_1$ state becomes effectively ligated during its first collision with the solvent. The branching ratio between spin crossover and ligation pathways is thus determined by the time of intra-molecular $^1A_1$ to $^3B_2$ SC with respect to solute-solvent collision frequency.

In conclusion, we would like to emphasize that further experimental studies are needed in order to fully understand the $Fe(CO)_4$ ligand exchange dynamics. These experiments should be able to clearly distinguish between different spin ($^1A_1$ vs. $^3B_2$) and coordination (complexed vs. uncomplexed) state of $Fe(CO)_4$. Femtosecond Fe L_3-edge RIXS technique utilized in the current study has this ability; however, a better time-resolution ($<$100 fs) and an improved signal-to-noise ratio are needed. Alternatively, recently developed combined ultrafast X-ray emission spectroscopy and diffuse X-ray scattering should also have this capability.[12,93] Additional difficulty related with the interpretation of these ultrafast, highly non-equilibrium processes is the fact that a relaxation to species with well-defined geometries and energy barriers has not yet taken place. This renders kinetic modeling of these processes approximate and it is thus anticipated that the analysis of the future improved experiments needs to consider the actual dynamical nature of these processes by taking into account the broad time-dependent distribution of structures the molecules are sampling.

ACKNOWLEDGMENTS

This work was supported by the Volkswagen Stiftung (M.B.), the Swedish Research Council (M.O.), the Carl Tryggers Foundation (M.O.), the Magnus Bergvall Foundation (M.O.), the Collaborative Research Centers SFB 755 and SFB 1073 (I.R., S.G., W.Q., M.S., and S.T.), and the Helmholtz Virtual Institute "Dynamic Pathways in Multidimensional Landscapes." W.Z., R.W.H., and K.J.G. acknowledge the support through the AMOS program within the Chemical Sciences, Geosciences, and Biosciences Division of the Office of Basic Energy Sciences, Office of Science, U.S. Department of Energy. Use of the Linac Coherent Light Source (LCLS), SLAC National Accelerator Laboratory, was supported by the U.S. Department of Energy, Office of Science, Office of Basic Energy Sciences under Contract No. DE-AC02-76SF00515. The SXR Instrument is funded by a consortium whose membership includes the LCLS, Stanford University through the Stanford Institute for Materials Energy Sciences (SIMES), Lawrence Berkeley National Laboratory (LBNL), University of Hamburg through the BMBF priority program FSP 301, and the Center for Free Electron Laser Science (CFEL). We thank Ryan Coffee, Greg Hays, Christian Weniger, Carlo Schmidt, and Erzsi Szilagyi for their support during the measurements at LCLS. We are grateful to Nils Mårtensson for making available the RIXS spectrometer and to Carl-Johan Englund, Markus Agåker, and Conny Såthe for helping to bring it into operation. We gratefully acknowledge Erik Nibbering's contribution to the LCLS beamtime proposal. The liquid jet end station was financed by Helmholtz Zentrum Berlin, the Max-Planck-Institute of Biophysical Chemistry, MAX-lab, and the Advanced Study Group of the Max Planck Society. The simulations were performed on resources provided by the Swedish National Infrastructure for Computing (SNIC) at the Swedish National Supercomputer Center (NSC), the High Performance Computer Center North (HPC2N),

and Chalmers Centre for Computational Science and Engineering (C3SE). We thank Werner Fuß for fruitful discussions.

[1]P. Wernet, K. Kunnus, I. Josefsson, I. Rajkovic, W. Quevedo, M. Beye, S. Schreck, S. Grübel, M. Scholz, D. Nordlund, W. Zhang, R. W. Hartsock, W. F. Schlotter, J. J. Turner, B. Kennedy, F. Hennies, F. M. F. de Groot, K. J. Gaffney, S. Techert, M. Odelius, and A. Föhlisch, Nature **520**, 78 (2015).
[2]J. Stöhr, *NEXAFS Spectroscopy* (Springer, Berlin, 1992).
[3]P. Wernet, Phys. Chem. Chem. Phys. **13**, 16941 (2011).
[4]C. Bressler, C. Milne, V.-T. Pham, A. ElNahhas, R. M. van der Veen, W. Gawelda, S. Johnson, P. Beaud, D. Grolimund, M. Kaiser, C. N. Borca, G. Ingold, R. Abela, and M. Chergui, Science **323**, 489 (2009).
[5]G. Vankó, P. Glatzel, V. T. Pham, R. Abela, D. Grolimund, C. N. Borca, S. L. Johnson, C. J. Milne, and C. Bressler, Angew. Chem., Int. Ed. **49**, 5910 (2010).
[6]N. Huse, H. Cho, K. Hong, L. Jamula, F. M. F. de Groot, T. K. Kim, J. K. McCusker, and R. W. Schoenlein, J. Phys. Chem. Lett. **2**, 880 (2011).
[7]B. E. Van Kuiken, N. Huse, H. Cho, M. L. Strader, M. S. Lynch, R. W. Schoenlein, and M. Khalil, J. Phys. Chem. Lett. **3**, 1695 (2012).
[8]B. Ahr, M. Chollet, B. Adams, E. M. Lunny, C. M. Laperle, and C. Rose-Petruck, Phys. Chem. Chem. Phys. **13**, 5590 (2011).
[9]H. T. Lemke, C. Bressler, L. X. Chen, D. M. Fritz, K. J. Gaffney, A. Galler, W. Gawelda, K. Haldrup, R. W. Hartsock, H. Ihee, J. Kim, K. H. Kim, J. H. Lee, M. M. Nielsen, A. B. Stickrath, W. K. Zhang, D. L. Zhu, and M. Cammarata, J. Phys. Chem. A **117**, 735 (2013).
[10]M. Dell'Angela, T. Anniyev, M. Beye, R. Coffee, A. Föhlisch, J. Gladh, T. Katayama, S. Kaya, O. Krupin, J. LaRue, A. Møgelhøj, D. Nordlund, J. K. Nørskov, H. Oberg, H. Ogasawara, H. Oström, L. G. M. Pettersson, W. F. Schlotter, J. A. Sellberg, F. Sorgenfrei, J. J. Turner, M. Wolf, W. Wurth, and A. Nilsson, Science **339**, 1302 (2013).
[11]W. Zhang, R. Alonso-Mori, U. Bergmann, C. Bressler, M. Chollet, A. Galler, W. Gawelda, R. G. Hadt, R. W. Hartsock, T. Kroll, K. S. Kjær, K. Kubiček, H. T. Lemke, H. W. Liang, D. A. Meyer, M. M. Nielsen, C. Purser, J. S. Robinson, E. I. Solomon, Z. Sun, D. Sokaras, T. B. van Driel, G. Vankó, T.-C. Weng, D. Zhu, and K. J. Gaffney, Nature **509**, 345 (2014).
[12]S. E. Canton, K. S. Kjær, G. Vankó, T. B. van Driel, S. Adachi, A. Bordage, C. Bressler, P. Chabera, M. Christensen, A. O. Dohn, A. Galler, W. Gawelda, D. Gosztola, K. Haldrup, T. Harlang, Y. Liu, K. B. Møller, Z. Németh, S. Nozawa, M. Pápai, T. Sato, T. Sato, K. Suarez-Alcantara, T. Togashi, K. Tono, J. Uhlig, D. A. Vithanage, K. Wärnmark, M. Yabashi, J. Zhang, V. Sundström, and M. M. Nielsen, Nat. Commun. **6**, 6359 (2015).
[13]M. Beye, F. Sorgenfrei, W. F. Schlotter, W. Wurth, and A. Föhlisch, Proc. Natl. Acad. Sci. U. S. A. **107**, 16772 (2010).
[14]T. Katayama, T. Anniyev, M. Beye, R. Coffee, M. Dell'Angela, A. Föhlisch, J. Gladh, S. Kaya, O. Krupin, A. Nilsson, D. Nordlund, W. F. Schlotter, J. A. Sellberg, F. Sorgenfrei, J. J. Turner, W. Wurth, H. Ostrom, and H. Ogasawara, J. Electron Spectrosc. Relat. Phenom. **187**, 9 (2013).
[15]M. Beye, T. Anniyev, R. Coffee, M. Dell'Angela, A. Föhlisch, J. Gladh, T. Katayama, S. Kaya, O. Krupin, A. Mogelhoj, A. Nilsson, D. Nordlund, J. K. Norskov, H. Oberg, H. Ogasawara, L. G. M. Pettersson, W. F. Schlotter, J. A. Sellberg, F. Sorgenfrei, J. J. Turner, M. Wolf, W. Wurth, and H. Ostrom, Phys. Rev. Lett. **110**, 186101 (2013).
[16]H. Öström, H. Oberg, H. Xin, J. LaRue, M. Beye, M. Dell'Angela, J. Gladh, M. L. Ng, J. A. Sellberg, S. Kaya, G. Mercurio, D. Nordlund, M. Hantschmann, F. Hieke, D. Kuhn, W. F. Schlotter, G. L. Dakovski, J. J. Turner, M. P. Minitti, A. Mitra, S. P. Moeller, A. Fohlisch, M. Wolf, W. Wurth, M. Persson, J. K. Norskov, F. Abild-Pedersen, H. Ogasawara, L. G. M. Pettersson, and A. Nilsson, Science **27**, 978 (2015).
[17]M. Dartigue, Y. Dartigue, and H. B. Gray, Bull. Soc. Chim. Fr. **12**, 4223 (1969).
[18]M. Kotzian, N. Rosch, H. Schroder, and M. C. Zerner, J. Am. Chem. Soc. **111**, 7687 (1989).
[19]J. T. Yardley, B. Gitlin, G. Nathanson, and A. M. Rosan, J. Chem. Phys. **74**, 370 (1981).
[20]O. Rubner, V. Engel, M. R. Hachey, and C. Daniel, Chem. Phys. Lett. **302**, 489 (1999).
[21]M. Wrighton, Chem. Rev. **74**, 401 (1974).
[22]M. S. Wrighton, D. S. Ginley, M. A. Schroeder, and D. L. Morse, Pure Appl. Chem. **41**, 671 (1975).
[23]N. Leadbeater, Coord. Chem. Rev. **188**, 35 (1999).
[24]M. Poliakoff and J. J. Turner, J. Chem. Soc. Faraday Trans. II **70**, 93 (1974).
[25]L. Bañares, T. Baumert, M. Bergt, B. Kiefer, and G. Gerber, Chem. Phys. Lett. **267**, 141 (1997).
[26]L. Bañares, T. Baumert, M. Bergt, B. Kiefer, and G. Gerber, J. Chem. Phys. **108**, 5799 (1998).
[27]S. K. Nayak and T. J. Burkey, Inorg. Chem. **31**, 1125 (1992).
[28]R. Ryther and E. Weitz, J. Phys. Chem. **95**, 9841 (1991).
[29]R. J. Ryther and E. Weitz, J. Phys. Chem. **96**, 2561 (1992).
[30]B. K. Venkataraman, G. Bandukwalla, Z. J. Zhang, and M. Vernon, J. Chem. Phys. **90**, 5510 (1989).
[31]S. A. Trushin, W. Fuß, K. L. Kompa, and W. E. Schmid, J. Phys. Chem. A **104**, 1997 (2000).
[32]M. Poliakoff and E. Weitz, Acc. Chem. Res. **20**, 408 (1987).
[33]E. Weitz, J. Phys. Chem. **91**, 3945 (1987).
[34]S. K. Nayak, G. J. Farrell, and T. J. Burkey, Inorg. Chem. **33**, 2236 (1994).
[35]P. Portius, J. Yang, X. Z. Sun, D. C. Grills, P. Matousek, A. W. Parker, M. Towrie, and M. W. George, J. Am. Chem. Soc. **126**, 10713 (2004).
[36]M. Besora, J. L. Carreón-Macedo, A. J. Cowan, M. W. George, J. N. Harvey, P. Portius, K. L. Ronayne, X. Z. Sun, and M. Towrie, J. Am. Chem. Soc. **131**, 3583 (2009).
[37]S. C. Nguyen, J. P. Lomont, M. C. Zoerb, A. D. Hill, J. P. Schlegel, and C. B. Harris, Organometallics **31**, 3980 (2012).
[38]S. P. Church, F.-W. Grevels, H. Hermann, J. M. Kelly, W. E. Klotzbucher, and K. Schaffner, J. Chem. Soc. Chem. Commun. **9**, 594 (1985).
[39]M. A. Schroeder and M. S. Wrighton, J. Am. Chem. Soc. **98**, 551 (1976).

[40]P. T. Snee, C. K. Payn, K. T. Kotz, H. Yang, and C. B. Harris, J. Am. Chem. Soc. **123**, 2255 (2001).
[41]P. T. Snee, C. K. Payne, S. D. Mebane, K. T. Kotz, and C. B. Harris, J. Am. Chem. Soc. **123**, 6909 (2001).
[42]M. Poliakoff and J. J. Turner, Angew. Chem., Int. Ed. **40**, 2809 (2001).
[43]H. Ihee, J. M. Cao, and A. H. Zewail, Angew. Chem., Int. Ed. **40**, 1532 (2001).
[44]A. L. Harris, J. K. Brown, and C. B. Harris, Ann. Rev. Phys. Chem. **39**, 341 (1988).
[45]R. M. Stratt and M. Maroncelli, J. Phys. Chem. **100**, 12981 (1996).
[46]C. G. Elles and F. F. Crim, Ann. Rev. Phys. Chem. **57**, 273 (2006).
[47]Y. Jiang, T. Lee, and C. G. Rose-Petruck, J. Phys. Chem. A **107**, 7524 (2003).
[48]J. Lessing, X. Li, T. Lee, and C. G. Rose-Petruck, J. Phys. Chem. A **112**, 2282 (2008).
[49]J. P. Lomont, S. C. Nguyen, and C. B. Harris, Acc. Chem. Res. **47**, 1634 (2014).
[50]W. F. Schlotter, J. J. Turner, M. Rowen, P. Heimann, M. Holmes, O. Krupin, M. Messerschmidt, S. Moeller, J. Krzywinski, R. Soufli, M. Fernandez-Perea, N. Kelez, S. Lee, R. Coffee, G. Hays, M. Beye, N. Gerken, F. Sorgenfrei, S. Hau-Riege, L. Juha, J. Chalupsky, V. Hajkova, A. P. Mancuso, A. Singer, O. Yefanov, I. A. Vartanyants, G. Cadenazzi, B. Abbey, K. A. Nugent, H. Sinn, J. Luening, S. Schaffert, S. Eisebitt, W.-S. Lee, A. Scherz, A. R. Nilsson, and W. Wurth, Rev. Sci. Instrum. **83**, 43107 (2012).
[51]G. L. Dakovski, P. Heimann, M. Holmes, O. Krupin, M. P. Minitti, A. Mitra, S. Moeller, M. Rowen, W. F. Schlotter, and J. J. Turner, J. Synchrotron Radiat. **22**, 498 (2015).
[52]K. Kunnus, I. Rajkovic, S. Schreck, W. Quevedo, S. Eckert, M. Beye, E. Suljoti, C. Weniger, C. Kalus, S. Grübel, M. Scholz, D. Nordlund, W. Zhang, R. W. Hartsock, K. J. Gaffney, W. F. Schlotter, J. J. Turner, B. Kennedy, F. Hennies, S. Techert, P. Wernet, and A. Föhlisch, Rev. Sci. Instrum. **83**, 123109 (2012).
[53]K. Tiedtke, A. A. Sorokin, U. Jastrow, P. Juranić, S. Kreis, N. Gerken, M. Richter, U. Arp, Y. Feng, D. Nordlund, R. Soufli, M. Fernández-Perea, L. Juha, P. Heimann, B. Nagler, H. J. Lee, S. Mack, M. Cammarata, O. Krupin, M. Messerschmidt, M. Holmes, M. Rowen, W. Schlotter, S. Moeller, and J. J. Turner, Opt. Express **22**, 21214 (2014).
[54]I. Josefsson, K. Kunnus, S. Schreck, A. Föhlisch, F. De Groot, P. Wernet, and M. Odelius, J. Phys. Chem. Lett. **3**, 3565 (2012).
[55]K. Kunnus, I. Josefsson, S. Schreck, W. Quevedo, P. S. Miedema, S. Techert, F. M. F. De Groot, M. Odelius, P. Wernet, and A. Föhlisch, J. Phys. Chem. B **117**, 16512 (2013).
[56]S. I. Bokarev, M. Dantz, E. Suljoti, O. Kühn, and E. F. Aziz, Phys. Rev. Lett. **111**, 83002 (2013).
[57]N. Engel, S. I. Bokarev, E. Suljoti, R. Garcia-Diez, K. M. Lange, K. Atak, R. Golnak, A. Kothe, M. Dantz, O. Kühn, and E. F. Aziz, J. Phys. Chem. B **118**, 1555 (2014).
[58]R. Pinjari, M. Delcey, M. Guo, M. Odelius, and M. Lundberg, J. Phys. Chem. **141**, 124116 (2014).
[59]P. Å. Malmqvist, A. Rendell, and B. O. Roos, J. Phys. Chem. **94**, 5477 (1990).
[60]E. Suljoti, R. Garcia-Diez, S. I. Bokarev, K. M. Lange, R. Schoch, B. Dierker, M. Dantz, K. Yamamoto, N. Engel, K. Atak, O. Kühn, M. Bauer, J. E. Rubensson, and E. F. Aziz, Angew. Chem., - Int. Ed. **52**, 9841 (2013).
[61]H. A. Kramers and W. Heisenberg, Z. Phys. **31**, 681 (1925).
[62]F. Gel'mukhanov and H. Ågren, Phys. Rev. A **49**, 4378 (1994).
[63]M. Ohno and G. A. van Riessen, J. Electron Spectrosc. Relat. Phenom. **128**, 1 (2003).
[64]F. Hennies, A. Pietzsch, M. Berglund, A. Föhlisch, T. Schmitt, V. Strocov, H. O. Karlsson, J. Andersson, and J. E. Rubensson, Phys. Rev. Lett. **104**, 193002 (2010).
[65]Y.-P. Sun, F. Hennies, A. Pietzsch, B. Kennedy, T. Schmitt, V. N. Strocov, J. Andersson, M. Berglund, J.-E. Rubensson, K. Aidas, F. Gel'mukhanov, M. Odelius, and A. Föhlisch, Phys. Rev. B **84**, 132202 (2011).
[66]CPMD, http://www.cpmd.org/, Copyright IBM Corp 1990–2008, Copyright MPI für Festkörperforschung Stuttgart 1997–2001.
[67]R. Car and M. Parrinello, Phys. Rev. Lett. **55**, 2471 (1985).
[68]B. R. Brooks, R. E. Bruccoleri, B. D. Olafson, D. J. States, S. Swaminathan, and M. Karplus, J. Comput. Chem. **4**, 187 (1983).
[69]W. L. Jorgensen, D. S. Maxwell, and J. Tirado-Rives, J. Am. Chem. Soc. **118**, 11225 (1996).
[70]S. Grimme, J. Comput. Chem. **27**, 1787 (2006).
[71]N. Troullier and J. L. Martins, Phys. Rev. B **43**, 1993 (1991).
[72]S. Goedecker, M. Teter, and J. Hutter, Phys. Rev. B **54**, 1703 (1996).
[73]See supplementary material at http://dx.doi.org/10.1063/1.4941602 for the complete results of the calculations and the rate models analysis (n.d.).
[74]C. Daniel, M. Benard, A. Dedieu, R. Wiest, and A. Veillard, J. Phys. Chem. **88**, 4805 (1984).
[75]W. Gawelda, A. Cannizzo, V. T. Pham, F. van Mourik, C. Bressler, and M. Chergui, J. Am. Chem. Soc. **129**, 8199 (2007).
[76]E. A. Juban, A. L. Smeigh, J. E. Monat, and J. K. McCusker, Coord. Chem. Rev. **250**, 1783 (2006).
[77]J. K. McCusker, Acc. Chem. Res. **36**, 876 (2003).
[78]M. Chergui, Acc. Chem. Res. **48**, 801 (2015).
[79]I. M. Waller and J. W. Hepburn, J. Chem. Phys. **88**, 6658 (1988).
[80]B. M. Fung and T. W. McGaughy, J. Chem. Phys. **65**, 2970 (1976).
[81]L. Saiz, J. A. Padro, and E. Guardia, J. Phys. Chem. B **101**, 78 (1997).
[82]J. A. Saxton, G. T. Coats, R. A. Bond, and R. M. Dickinson, J. Chem. Phys. **37**, 2132 (1962).
[83]S. E. Bromberg, H. Yang, M. C. Asplund, T. Lian, B. K. McNamara, K. T. Kotz, J. S. Yeston, M. Wilkens, H. Frei, R. G. Bergman, and C. B. Harris, Science **278**, 260 (1997).
[84]M. Brookhart, M. L. H. Green, and G. Parkin, Proc. Natl. Acad. Sci. U. S. A. **104**, 6908 (2007).
[85]J. D. Simon and X. Xie, J. Phys. Chem. **90**, 6751 (1986).
[86]A. G. Joly and K. A. Nelson, J. Phys. Chem. **93**, 2876 (1989).
[87]A. G. Joly and K. A. Nelson, Chem. Phys. **152**, 69 (1991).
[88]K. T. Kotz, H. Yang, P. T. Snee, C. K. Payne, and C. B. Harris, J. Organomet. Chem. **596**, 183 (2000).
[89]J. D. Simon and X. Xie, J. Phys. Chem. **93**, 291 (1989).
[90]X. Xie and J. D. Simon, J. Am. Chem. Soc. **112**, 1130 (1990).

[91]T. P. Dougherty and E. J. Heilweil, Chem. Phys. Lett. **227**, 19 (1994).
[92]T. Q. Lian, S. E. Bromberg, M. C. Asplund, H. Yang, and C. B. Harris, J. Phys. Chem. **100**, 11994 (1996).
[93]C. Bressler, W. Gawelda, A. Galler, M. M. Nielsen, V. Sundström, G. Doumy, A. M. March, S. H. Southworth, L. Young, and G. Vankó, Faraday Discuss. **171**, 169 (2014).